https://doi.org/10.5194/tc-2021-301
Preprint. Discussion started: 25 October 2021
© Author(s) 2021. CC BY 4.0 License.

The Cryosphere Discussions
Open Access
EGU

Antarctic Peninsula ice shelf collapse triggered by föhn wind-induced melt

Matthew K. Laffin[1], Charles S. Zender[1,2], Melchior van Wessem[3], Sebastián Marinsek[4]

[1]Department of Earth System Science, University of California, Irvine
[2]Department of Computer Science, University of California, Irvine
[3]Institute for Marine and Atmospheric Research Utrecht (IMAU), Utrecht University
[4]Instituto Antártico Argentino, Buenos Aires, Argentina

Correspondence to: Matthew K. Laffin (mlaffin@uci.edu)

Abstract. Ice shelf collapse reduces buttressing and enables glaciers to contribute more rapidly to sea-level rise in a warming climate. The abrupt collapses of the Larsen A and B ice shelves on the Antarctic Peninsula (AP) have been attributed to increased surface melt. However, no studies examine the timing, magnitude, and location of surface melt processes immediately preceding these disintegrations. Here we use a regional climate model and Machine Learning analyses to evaluate the influence of föhn wind events on the surface liquid water budget for collapsed and extant ice shelves. We find föhn winds caused 25% of the total annual melt in just 9 days on Larsen A which helped melt lakes surpass a critical stability depth that, we suggest, ultimately triggered collapse. By contrast, föhns appear to pre-condition, not trigger, Larsen B's collapse. AP extant ice shelves will remain less vulnerable to surface-melt-driven instability due to weaker föhn-driven melt so long as surface temperatures and föhn occurrence remain within historical bounds.

1 Introduction

The sudden disintegration of ice shelves on the eastern periphery of the Antarctic Peninsula (AP) represents the culmination of a critical regional warming trend and anomalous surface melt in the region (Vaughan et al., 2003). Forensic examination of surface melt on ice shelves, which subdue the discharge of grounded ice into the global ocean, can lead to improved projections of sea-level rise (Rignot et al., 2004; Gudmundsson et al., 2013; Borstad et al., 2016). Enhanced regional temperatures and associated surface meltwater are considered the leading contributors to the final stages of the Larsen A and B ice shelf collapses (Van Den Broeke et al., 2005; Trusel et al, 2013), and have received considerable scientific attention, but the detailed mechanisms that melt the surface, and the rate and timing of surface melt, particularly föhn wind-induced have not been examined in complete detail. Here, using Machine Learning (ML) methods to identify föhn events we document the existence of strong föhn jets and increased surface melt rates preceding the final collapse events and assess the

https://doi.org/10.5194/tc-2021-301
Preprint. Discussion started: 25 October 2021
© Author(s) 2021. CC BY 4.0 License.


significance of the föhn-melt mechanism for the stability of the remaining eastern AP ice shelves. Our ML method is the most accurate method to identify föhn winds, and when combined with regional climate model output produces the most accurate melt mechanism quantification.

The final collapses of the Larsen A (LAIS) in 1995 and the Larsen B (LBIS) ice shelves in 2002 have been attributed to decreased structural integrity brought on by a combination of factors. Most notably, regional atmospheric warming (Scambos et al., 2000; Mulvaney et al., 2012), extended melt seasons (Scambos et al., 2003), multi-year firn pore space depletion (Kuipers Munneke et al., 2012; Trusel et al., 2015), melt pond flooding and crevasse expansion through hydrofracture (Scambos et al., 2003; Pollard et al., 2015; Banwell et al., 2019; Robel and Banwell, 2019), glacier structural discontinuities (Glasser et al., 2008), basal melt (Pritchard et al., 2012; Rignot et al., 2013; Depoorter et al., 2013; Schodlok et al., 2016; Adusumilli et al., 2016), warm melt-water intrusion (Braun et al., 2009), melting of the ice melange within rifts conducive to rift propagation (Poinelli et al., 2021), and regional sea ice loss allowing ocean swell flexure stress on the calving front (Massom et al., 2018). Satellite observations and ice shelf stability model studies have determined the LBIS was covered with >2750 melt lakes that were on average 1 meter deep before collapse which corresponds to a possible melt lake depth of stability threshold for ice shelves in the region (Glasser et al., 2008; Banwell et al., 2013). Ice shelves inundated with surface melt lakes are susceptible to disintegration through a process known as hydrofracture, where meltwater applies outward and downward pressure to the walls and tip of crevasses that can propagate through the ice shelf (Scambos et al., 2003; Banwell et al., 2013; Bell et al., 2018). Melt lakes at critical water depths create a fracture pattern that splits ice shelves into sections with aspect ratios that support unstable rollover and hydrofracture cascades that begin when melt lakes drain or calving occurs at the ice shelf terminus (Banwell et al., 2013; Robel et al., 2019).

Previous research acknowledges enhanced surface melt during years of collapse and the presence of föhn wind events in the region, however, no attempt to produce a timeline of total melt quantity or melt caused by föhn before and during ice shelf breakup has been undertaken. Before and during the final stage of the collapse events, satellite observations indicate numerous surface melt lakes and a sky generally clear of clouds (Figure 1b-f). Clear skies are one indicator that high melt rate northwesterly downslope föhn winds may have been present during the collapse events (Elvidge et al., 2020; Laffin et al., 2021). Although the AP is one of the fastest-warming regions on Earth there have been no additional sudden collapse events on the eastern AP since 2002 (Vaughan et al., 2003; Bozkurt et al., 2020). The questions, therefore, arise: 1) To what extent does föhn-induced melt contribute to the surface melt budget on the AP?; 2) Does the confluence of föhn-induced melt quantity, spatial impact, and timing constitute a trigger for the collapse of the LAIS and LBIS?; 3) What are the implications of föhn-induced melt for the remaining eastern AP ice shelves?

To address these questions we consider three metrics: Section 3.1 explores the total annual melt quantity and spatial distribution caused by föhn winds.; Section 3.2 identifies the coincidence of föhn-induced melt preceding and during the collapse events, and the estimated melt lake depth in response to melt events.; Section 3.3 identifies the contribution of föhn

https://doi.org/10.5194/tc-2021-301
Preprint. Discussion started: 25 October 2021
© Author(s) 2021. CC BY 4.0 License.

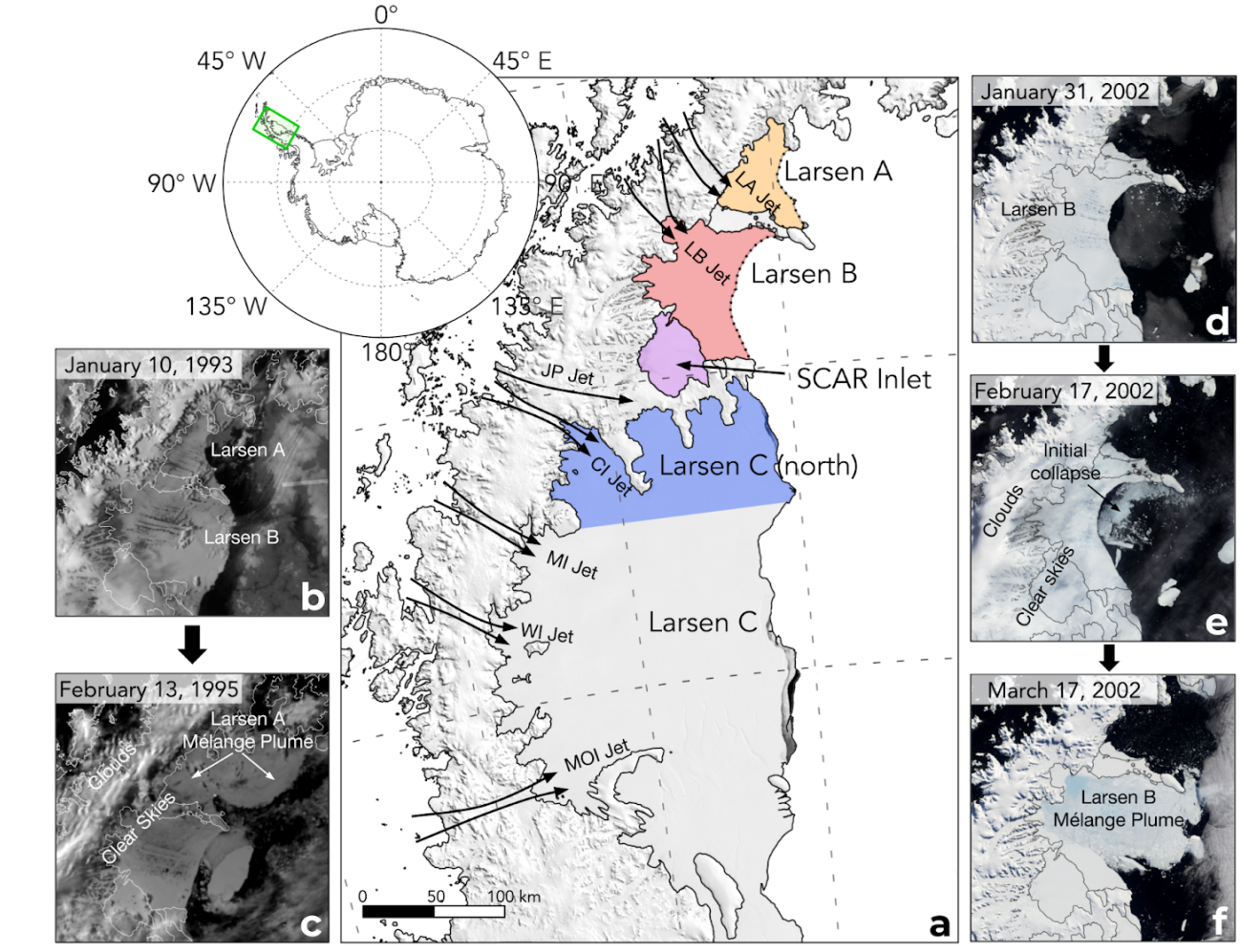

Figure 1. Map of the northern Antarctic Peninsula (a) showing locations of ice shelves and föhn jets (Larsen A jet (LA jet), Larsen B jet (LB jet), Jason Peninsula jet (JP jet), Cabinet inlet jet (CI jet), Mill inlet jet (MI jet), Whirlwind inlet jet (WI jet), Mobil Oil inlet jet (MOI jet)) with a MODIS Mosaic overlay. The colors indicate how this study separates ice shelves for analysis. The dotted lines show the former extent of the Larsen A and Larsen B ice shelves at the time of collapse. Panels (b)-(f) are satellite images of the collapses of the LAIS and LBIS. (b) AVHRR (Advanced Very High-Resolution Radiometer) image of the northern AP two years before the collapse of the LAIS showing melt lakes on the surface of both ice shelves. (c) AVHRR image after the collapse of the LAIS. (d) MODIS (Moderate Resolution Imaging Spectroradiometer) image showing the LBIS days before collapse began. (e) MODIS image showing a föhn wind event (clouds

https://doi.org/10.5194/tc-2021-301
Preprint. Discussion started: 25 October 2021
© Author(s) 2021. CC BY 4.0 License.


over the western AP, clear skies over the ice shelves) along with the initial collapse of the LBIS. (f) MODIS image of the complete collapse of the LBIS.

2 Data and methods

2.1 Regional Climate Model Data (RACMO2)

We base our analysis on 3-hourly output from simulations by the Regional Atmospheric Climate Model 2 (RACMO2), version 2.3p2, with a horizontal resolution of 5.5km (0.05°) focused on the AP from 1979-2018. RACMO2 uses the physics package CY33r1 of the ECMWF Integrated Forecast System (IFS) (https://www.ecmwf.int/en/elibrary/9227-part-iv-physical-processes\textit{{ECMWF-IFS,} 2008}) in combination with atmospheric dynamics of the High-Resolution Limited Area Model (HIRLAM). RACMO2 has been evaluated against numerous surface observations (AWS) in locations all over the AP and has trouble simulating very high and low-temperature extremes in the region but is considered a good representation of surface conditions (Leeson et al., 2017; Laffin et al., 2021).

2.2 Föhn wind detection

We developed a Föhn Detection Algorithm (FöhnDA) that identifies föhn winds that cause melt using 12 Automatic Weather Stations (AWS) on the AP as detailed in Laffin et al., (2021). FöhnDA identifies föhn-induced melt events using binary classification when air temperature (T) is greater than 0°C, which ensures it captures föhn events that cause surface melt. Thresholds for relative humidity (RH) and wind speed (WS) are more dynamic because high wind speeds and low relative humidity do not guarantee temperatures above freezing, they only aid to identify föhn. FöhnDA uses quantile regression to identify these variable thresholds that take into account the climatology and seasonality at each weather station site. FöhnDA uses two empirically determined thresholds: the 60th percentile wind speed and 30th percentile relative humidity which are 2.85 m/s and 79% averaged at all AWS locations. We co-locate AWS with the nearest model grid cell and use FöhnDA results to train an ML model that detects föhn winds in RACMO2 output. Our ML model improves the accuracy of föhn detection by over 23% when compared to the simple binary classification method applied to RACMO2 output as described above. This method is the most accurate detection method compared to previous work and allows us to use in situ observations from AWS and expand föhn detection with RACMO2 output to regions and times when AWS observations are not available (Figure S2).

Föhn jet locations were identified using wind direction and strength during föhn events (Figure 2a) and by the surface melt pattern during föhn (Figure 3b). The RACMO2 topography pixel size is 5.5 km which is sufficient to produce the föhn jets identified on the LCIS (Elvidge et al., 2015), and allows for new föhn jet identification on the LAIS and LBIS despite lack of direct observation.. However, small-scale föhn winds funneled through local canyons and mountain gaps

https://doi.org/10.5194/tc-2021-301
Preprint. Discussion started: 25 October 2021
© Author(s) 2021. CC BY 4.0 License.


smaller than 5.5 km are not directly simulated. Therefore, we consider RACMO2 simulated estimates of surface melt caused by föhn winds to be conservative and likely higher in regions where föhn winds are funneled and concentrated.

2.3 Ice shelf intercomparison analysis

We split each of the five ice shelves shown in Figure 1a and take the average of all model grid cells annually to create a climatology of surface melt, melt rate, melt hours, surface temperature. We use a two-tailed t-test statistic to identify if the mean of both ice shelves is statistically different from one another at the 95% confidence interval. We compare all ice shelves to the LBIS because it was the most recent collapse event and is adjacent to collapsed and existing ice shelves. Qualitatively similar results are obtained when comparing all ice shelves to the LAIS.

3 Results

3.1 Föhn jets and melt

Using RACMO2 historical simulations, informed by a Machine Learning algorithm that is trained with Automatic Weather Station (AWS) observations (Laffin et al., 2021), we identify seven recurring föhn jets or gap winds that lead to high surface melt rates on the eastern AP ice shelves (Figure 2a). Four of these jets (CI, MI, WI, MOI) have been studied using airborne observations and model simulations (Grosvenor et al., 2014; Elvidge et al., 2016). The remaining three jets (LA, LB, and JP) are, to our knowledge, identified here for the first time. Föhn winds form when moist air is forced over a mountain barrier, often leading to precipitation on the windward side of the barrier that dries the air mass (Elvidge et al., 2016). As the now drier air descends the leeward slope it warms adiabatically and promotes melt directly through sensible heat exchange, and indirectly by the associated clear skies that allow additional shortwave radiation to reach the surface in non-winter months (Elvidge et al., 2020; Laffin et al., 2021). These positive energy balance components increase surface melt rates up to 54% relative to non-föhn induced melt (Figure 2b). Additionally, AP winds from the west and northwest (föhn influence) produce surface melt rates twice as large as the average melt rate from all other wind directions (Figure 2c).

https://doi.org/10.5194/tc-2021-301
Preprint. Discussion started: 25 October 2021
© Author(s) 2021. CC BY 4.0 License.

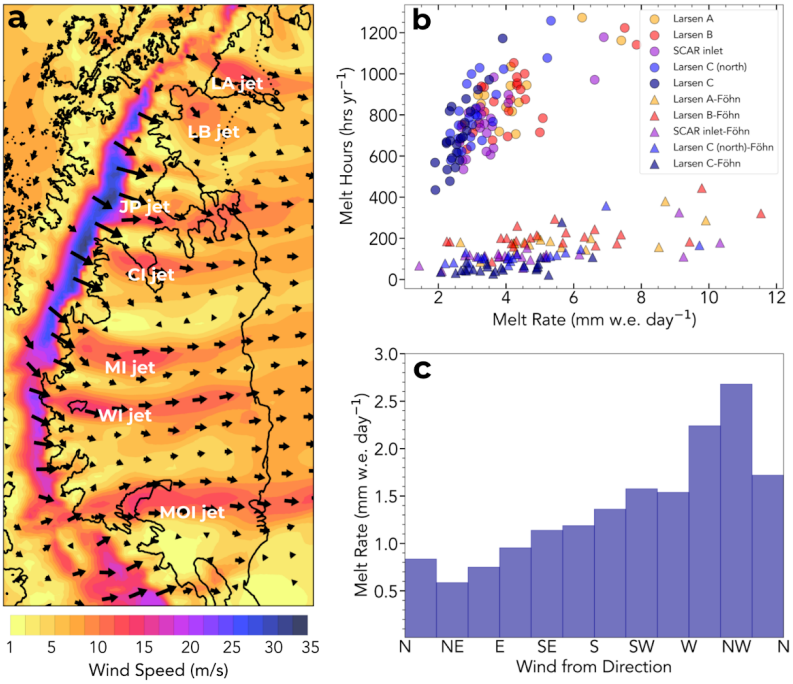

Figure 2. (a) The northern AP showing the RACMO2-simulated wind speed and direction vectors on January 24, 1995, just before the collapse of the LAIS. Föhn jet locations are indicated with names. (b) Annual surface melt hours and melt rate on each ice shelf during föhn (triangle) and non-föhn (circle) melt from 1980-2002. (c) Melt rate as a function of wind direction averaged for all ice shelves on the AP from 1980-2002.

The degree to which föhn winds impact surface melt on each ice shelf varies, and provides insight into why SCAR inlet and the LCIS remain intact while the LAIS and LBIS have collapsed other than the significant difference in annual surface temperature (Figure 5). Surface melt production is pronounced under the influence of föhn jets, particularly for the LA and LB jets which produce 35.7% and 31.8% more melt respectively compared to regions not in the path of a föhn jet on the ice shelves (Figure 3). Föhn-induced surface melt accounts for 32% of the total annual melt between 1979 and 2002 on the LAIS and 47% of total melt on the LBIS (Figure 3c). In locations directly influenced by föhn jets, the mean annual föhn-induced melt was as high as 61% on the LAIS and 57% on the LBIS of total annual melt. By contrast, föhn-induced melt accounts for only 24% of 1979-2002 total melt on SCAR inlet and 17% on the LCIS. SCAR inlet is not directly impacted by a föhn jet, but still experiences weak föhn influence and clear skies. The LCIS is affected by numerous föhn jets (CI, MI, WI, MOI), accounting for up to 40% of the total annual melt in Cabinet and Whirlwind inlets, decreasing with distance east of the AP mountains. The stark contrast in surface melt amount and fraction caused by föhn winds on collapsed vs. intact ice shelves implicates föhn melt as a contributor to the LAIS and LBIS collapses. However, no single factor,

https://doi.org/10.5194/tc-2021-301
Preprint. Discussion started: 25 October 2021
© Author(s) 2021. CC BY 4.0 License.


including föhn-induced melt rate, lessens the influence of all the other factors that contributed to these collapses. A clearer picture of the role of föhns emerges after we examine föhn-induced melt extent and timing.

The spatial distribution and extent of surface melt influence ice shelf stability. Surface melt and melt lakes near the ice shelf terminus can lead to calving front collapse and structural instability for the remaining portion of the ice shelves (Depoorter et al.,2013; Pollard et al., 2015). Consistent with this mechanism, the LA and LB föhn jets impact a large spatial area of the LAIS and LBIS, and reach the ice shelf calving fronts (Figure 3b). SCAR Inlet lacks a strong föhn jet/influence and does not regularly experience largescale melt lakes even during high melt years (Figure 1b-f). This helps explain why SCAR Inlet is still intact, despite major structural changes observed after the collapse of the LBIS (Borstad et al., 2016; Qiao et al., 2020). LCIS on the other hand is impacted by four major jets and regularly experiences föhn-induced melt lakes, particularly in Cabinet inlet. However, the vast size of the LCIS does not allow the föhn-induced melt to reach the terminus. The föhn melt mechanism breaks down by mixing with cold air which reduces the intensity of the föhn jets from their peak at the base of the AP mountains to the calving front (Figure 3b). Having established that föhn winds significantly enhanced surface melt overall and at the crucial calving front of LAIS and LBIS, we now examine the timing of föhn-induced melt events relative to the collapses.

https://doi.org/10.5194/tc-2021-301
Preprint. Discussion started: 25 October 2021
© Author(s) 2021. CC BY 4.0 License.

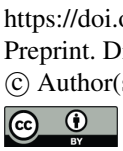

The Cryosphere Discussions
Open Access
EGU

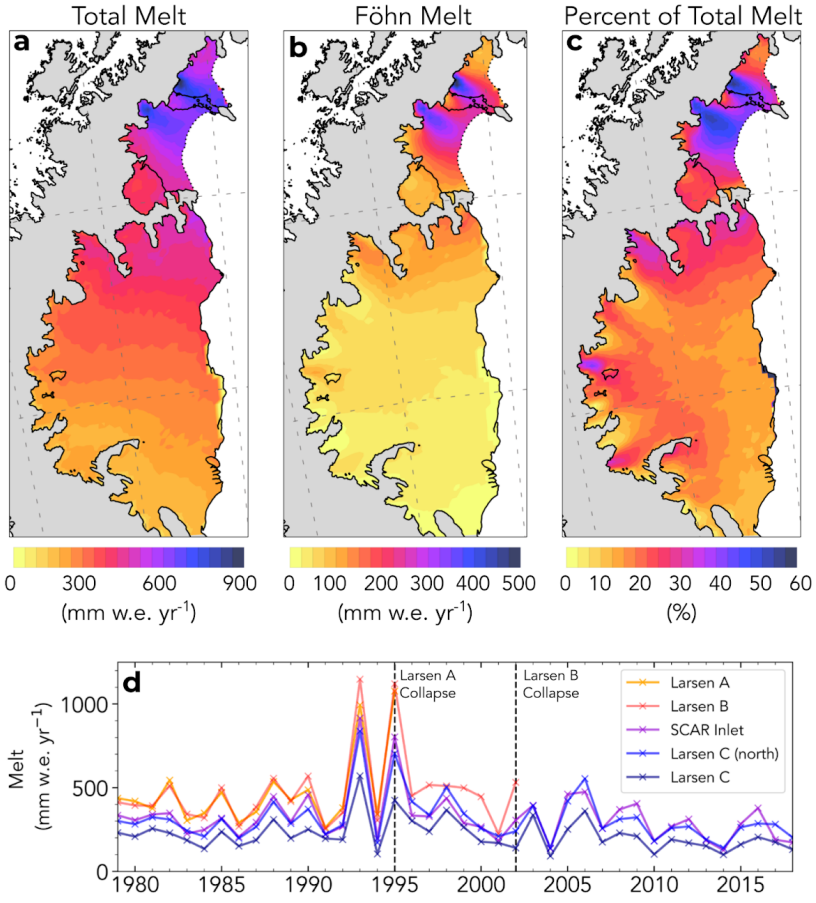

Figure 3. (a) Average annual melt from 1980-2002. (b) Average annual föhn wind-induced melt from 1980-2002. (c) Percent of total melt concurrent with föhn wind from 1980-2002. (d) Time series of the mean annual surface melt on each ice shelf from 1979-2018. Dashed vertical lines indicate the year in which each ice shelf collapsed. Note: The Larsen B curve often overlaps the Larsen A curve.

3.2 Coincidence of föhn winds with collapse

3.2.1 LAIS

Three föhn wind events occurred on LAIS between January 18 and 27, 1995, overlapping with the initial phase of the LAIS collapse that began on January 25 (Figure 4b) (Rott et al., 1998). These föhn events lasted an average of 3 days each and produced increased surface melt greater than any other 9 day period from 1979-2018, with mean cumulative melt of 268.5 mm w.e. or 25.2% of the total annual melt in the 1994/95 melt season. Total melt during the 1994/95 melt season was 127% higher than an average year (474 mm w.e./yr) and the 9-day föhn wind event produced 57% of the total melt of an average melt year. Therefore this 9-day föhn-induced melt event and melt year are clearly anomalous in the observational record.

https://doi.org/10.5194/tc-2021-301
Preprint. Discussion started: 25 October 2021
© Author(s) 2021. CC BY 4.0 License.


We next examine the contribution of föhn-generated melt to other observables implicated in the collapse, namely surface liquid water, melt lake depth, and melt lake extent (Scambos et al., 2003; Banwell et al., 2013). We estimate the spatial extent and depth of melt lakes prior to collapse on the LAIS using satellite images of melt lake surface area combined with model-simulated available liquid water volume. The cumulative spatial melt pattern between January 18 and 27, 1995 identifies significant melt on the LAIS ranging from 157-356 mm w.e. (Figure S1a), varying spatially with the influence of the LA jet. Satellite imagery of the LAIS during collapse does not yield high enough resolution to decipher melt lake surface area however Advanced Very High-Resolution Radiometer (AVHRR) imagery on December 8, 1992, provides high-resolution cloudless images of the ice shelf taken at the end of a similar föhn-induced melt event during a year when melt was comparable to the 1994/95 melt season, therefore we consider this melt lake extent analogous to the 1994/95 melt season (Figure 4a). We find the melt lake surface area was likely between 5.1%-10.8% (103 km2 - 219 km2) of the total LAIS surface area (Figure S1b). Melt lake surface area is likely underestimated because the image was taken early in the 1992/93 melt season and does not easily identify small lakes or river systems. Liquid water pooling on the ice surface is modulated by the local topography. If we assume all the available surface liquid water during the 9-day melt period, minus evaporation, runoff, and refreeze, forms lakes that cover the same estimated surface area as the 1992/93 melt season, we can estimate melt lake depth during the initial collapse. We find mean melt lake depth to be between 1.38-6.86 meters depending on lake location and föhn influence, which exceeds the average lake depth of the LBIS lakes prior to collapse (1 meter) and the critical lake depth that was identified in LBIS collapse modeling studies (3.5 m), especially under the influence of the LA jet (Banwell et al., 2013).

3.2.2 LBIS

A föhn wind event coincided with the initial LBIS collapse on February 9, 2002, with complete collapse by March 17, 2002 (Figure 4c). In contrast to föhn pre-cursors of the LAIS collapse, föhn events in the LBIS 2001/02 melt season were relatively short, averaging less than 24 hours per event, and produced melt rates just 27% higher than non-föhn melt that year and only 39% of the average föhn melt rate in all other years (Figure 4e). We conclude that while enhanced surface melt from föhn winds likely triggered the LAIS collapse, the LBIS collapse was not directly related to the impact of föhn-induced melt. Nevertheless, previous high melt rate föhn events such as those in the 1992/93 and 1994/95 melt seasons likely preconditioned the LBIS through firn densification to support melt lake formation, discussed in section 3.3.

https://doi.org/10.5194/tc-2021-301
Preprint. Discussion started: 25 October 2021
© Author(s) 2021. CC BY 4.0 License.

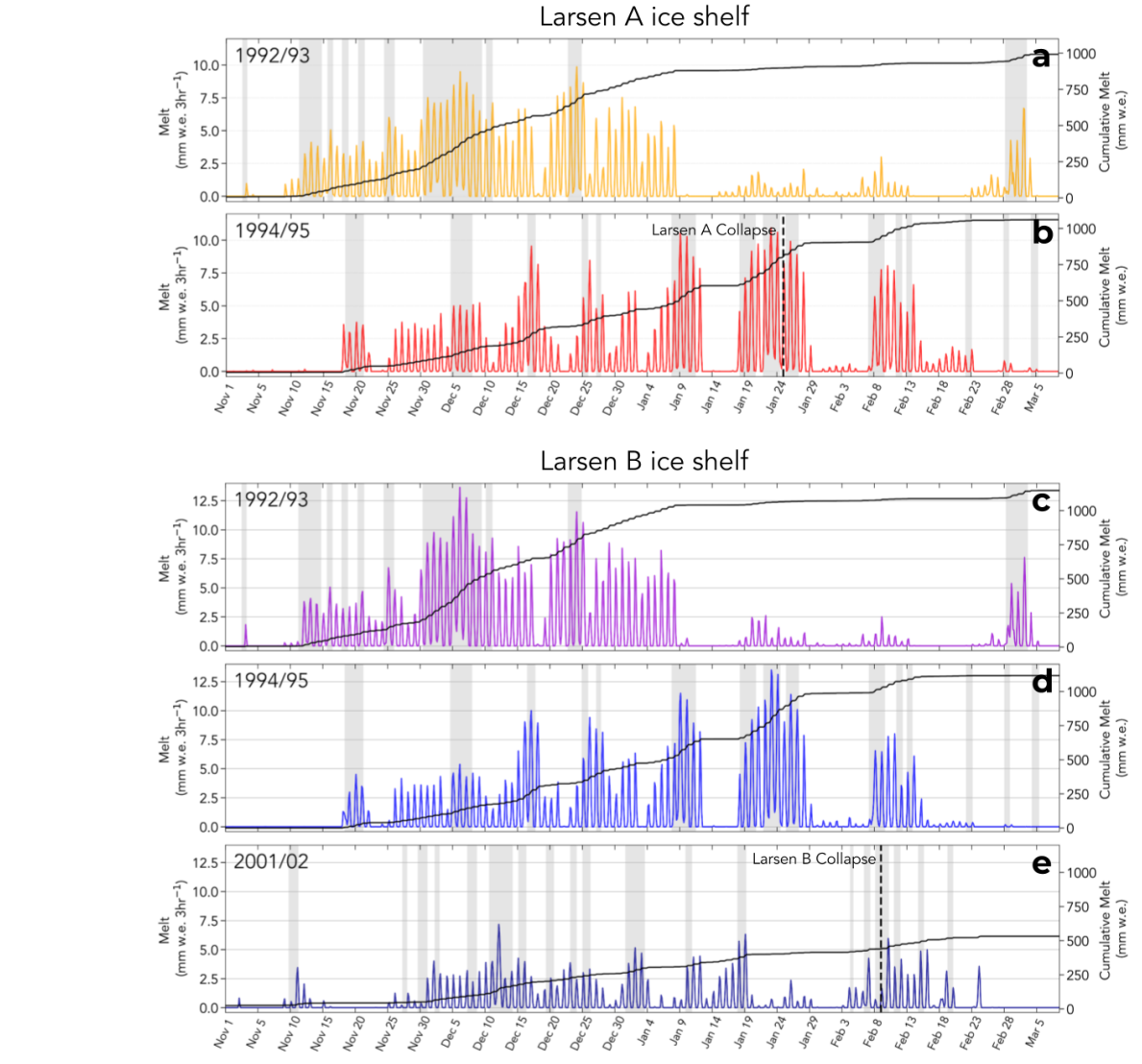

Figure 4. Time series of surface melt production and cumulative melt during the Antarctic melt season averaged over the indicated ice shelf. Grey shading indicates the presence of föhn winds. (a) 1992/1993 LAIS. (b) 1994/1995 LAIS. (c) 1992/1993 LBIS. (d) 1994/1995 LBIS. (e) 2001/2002 LBIS. *Note*: Surface melt that occurs after the collapse events indicated by the dashed vertical lines in (b) and (e) are estimates of melt quantity if the ice shelves did not disintegrate.

3.3 Föhn melt and the surface liquid water budget

To better understand the role that föhn winds have played in AP ice shelf surface melt and stability we intercompare melt climatologies of all major ice shelves. Comparing collapsed with intact ice shelves yields a clearer picture of the effects föhn winds have on ice shelf stability. We identify whether annual surface melt production, melt rate, melt hours, and surface

https://doi.org/10.5194/tc-2021-301
Preprint. Discussion started: 25 October 2021
© Author(s) 2021. CC BY 4.0 License.


temperature variables from 1980-2002 are significantly different from the LBIS (Figure 5 and corresponding two-tailed t-test statistics in Table S1). We compare to LBIS because it was centered between other ice shelves and was the most recent to collapse. Total surface melt production on every ice shelf except LAIS differs significantly from LBIS melt (Mean annual melt; LAIS-476 mm w.e., LBIS-479 mm w.e., SCAR-353 mm w.e., Larsen(north)-336 mm w.e., LCIS-238 mm w.e.) (Figure 5a), which is expected when we consider the latitudinal location and mean annual air temperature (Figure 5d) (Table S1). However, when föhn-induced melt is subtracted from total melt, the mean annual surface melt production on SCAR inlet and Larsen C (north) are not statistically different from the LBIS (LAIS-337 mm w.e., LBIS-321 mm w.e., SCAR-286 mm w.e., Larsen(north)-278 mm w.e., LCIS-203 mm w.e.) (Figure 5b). In other words, with the exception of föhn-induced melt (Figure 5c), melt production on SCAR Inlet and LCIS are statistically indistinguishable at the 95% confidence interval from LBIS melt production. Föhn wind-induced surface melt impacted the collapse significantly more than extant ice shelves further implicates föhn melt as an important contributor to LAIS and possibly LBIS collapse. The relatively small role that föhns play in the liquid water production and variability on the remaining ice shelves bodes well for their continued resilience.

The nominal amount of föhn-induced melt on the LBIS in the 2001/02 melt season nevertheless played a role in ice shelf stability through firn densification. Firn densification occurs when the liquid water fills the pore space between snow/ice crystals decreasing the air content in the firn, which forms refrozen ice layers that promote melt lake formation (Kuipers Munneke et al., 2012; Polashenski et al., 2017). A liquid-to-solid ratio (LSR) is a crude proxy for available firn air content and can be estimated as,

$$LSR = \frac{Total\ liquid\ water\ (snowmelt + liquid\ precipitation)}{Total\ solid\ precipitation\ (snow)} \quad (1)$$

where areas with LSR < 1 represent an ice shelf that receives more solid precipitation than liquid water and is therefore less likely to saturate with liquid water and form melt lakes than areas with LSR > 1 (Figure 6). Extant ice shelves (SCAR inlet, LCIS) have an LSR just above 1 for the period 1980-2002 if all surface melt is included (Figure 6a). The LSR for LAIS and LBIS is also just above 1 for this period, though only if föhn-induced surface melt is excluded. However, when surface melt caused by föhn wind is included, LSR exceeds 1.5 throughout extensive regions, including the ice shelf margins, of the LAIS and LBIS. Thus the collapsed ice shelves experienced climatological LSRs significantly larger than the extant ice shelves, mainly due to föhn-induced melt. This again suggests that föhn-induced melt helped precondition the LAIS and LBIS to collapse by long-term firn densification.

https://doi.org/10.5194/tc-2021-301
Preprint. Discussion started: 25 October 2021
© Author(s) 2021. CC BY 4.0 License.

The Cryosphere Discussions
Open Access
EGU

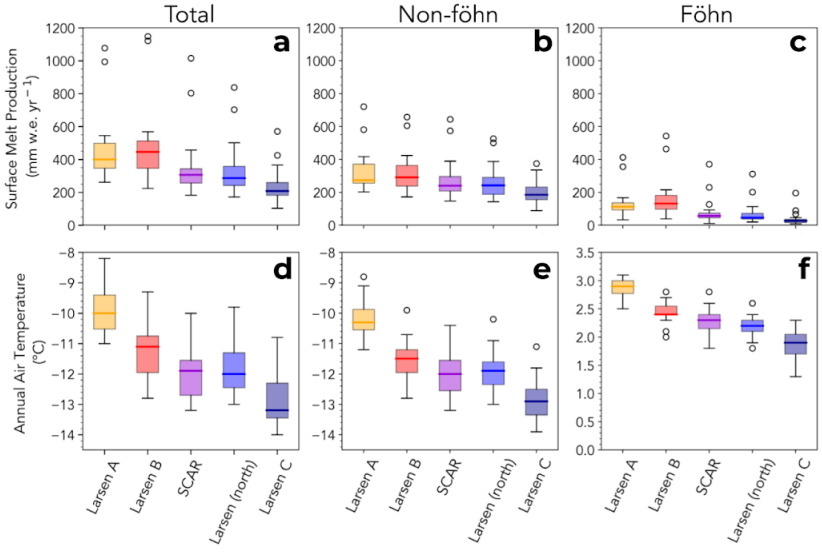

Figure 5. Box and whisker plots intercompare ice shelves with data from 1980-2002. Annual surface melt production (a) all melt, (b) non-föhn melt, (c) föhn-induced melt. (d) Mean annual air temperature, (e) air temperature without föhn winds, (f) air temperature during föhn winds. *Note*: the LAIS estimates are hypothetical after 1995, but are still resolved in the model simulations.

235

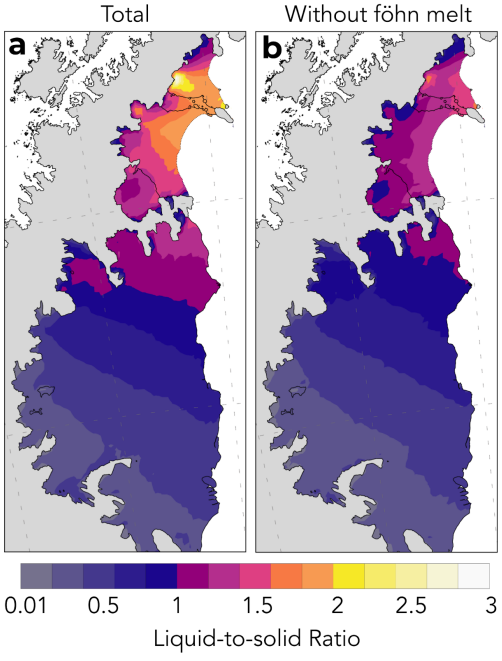

Figure 6. Firn liquid-to-solid ratio or mean annual liquid water divided by mean annual frozen precipitation for (a) total and (b) all liquid water except föhn-induced melt. *Note*: the LAIS estimates are hypothetical after 1995, but are still resolved in the model simulations.

https://doi.org/10.5194/tc-2021-301
Preprint. Discussion started: 25 October 2021
© Author(s) 2021. CC BY 4.0 License.


4 Discussion

It is reasonable to expect differences in ice shelf melt regime, particularly with the north/south temperature gradient present on the eastern AP ice shelves. The annual surface temperature difference between ice shelves could explain ice shelf disintegration through long-term thinning and retreat (Scambos et al., 2003; Morris et al., 2003), however, temperature gradient alone cannot explain the substantial increase in surface melt on the LAIS and LBIS. Only with the addition of föhn-induced surface melt do the LAIS and LBIS stand out significantly from the other eastern AP ice shelves. With that in mind, we have examined liquid water processes on the spatio-temporal scales pertinent to AP ice shelf stability. For instance, the structural flow discontinuities or suture zones, where tributary glaciers merge together to form an ice shelf, are mechanically weak points that impact stability (Glasser et al., 2008). These suture zones are further weakened through lateral shear depending on the difference in tributary glacier flow. All ice shelves in the region are comprised of numerous outflow glaciers sutured together, and while some studies suggest this is a major contributor to ice shelf instability, only two of the ice shelves have collapsed (Borstad et al., 2016; Glasser et al., 2008; Glasser et al., 2021). Further research suggests that marine accretion of ice on the bottom of the ice shelves, specifically LCIS, may stabilize these suture zones, which may be why SCAR inlet has remained intact despite major rift formation (McGrath et al., 2014; Borstad et al., 2016).

The timing of surface melt and melt enhanced by föhn winds within the melt season provides insight into the fate of LAIS and LBIS, including why neither ice shelf collapsed in the anomalously strong 1992/93 melt season (Figure 3d). Pore space within the upper snow and firn layers buffers surface melt before lakes begin to form (Polashenski et al., 2017). Late season melt is more likely to form surface melt lakes because meltwater from the preceding fall, winter, and spring has partially or completely filled available pore space. On both the LAIS and LBIS, 92% of surface melt during the 1992/93 melt season occurred before January 9th when there was more pore space to buffer the anomalous surface melt than at the onsets of their collapses in late January 1995 and early February 2002, respectively (Figure 4a, c). Melt lakes were present on both ice shelves throughout the 1992/93 melt season, though melt production slowed dramatically after mid-January, 1993 (Scambos et al., 2000). The high melt rates in late November and early December 1992 on the LAIS were perhaps too early in the melt season, and after too many years of nominal melt, to form substantial melt lakes and trigger hydrofracture that season. Nevertheless, the 1992/93 melt could have preconditioned the shelf for collapse in January 1995. The LBIS collapse began in February 2002 after the surface melt had returned to nominal, 1980s levels for six years. How much pore space had recovered during those six years is unknown, and an important question for future research. Satellite images of surface melt lakes indicate 11% of the ice shelf was covered in melt lakes prior to collapse (Glasser et al., 2008). However, the preceding melt year (2000/2001) had low melt and high precipitation, which added additional snow mass to the unstable ice shelf (Leeson et al., 2017).

https://doi.org/10.5194/tc-2021-301
Preprint. Discussion started: 25 October 2021
© Author(s) 2021. CC BY 4.0 License.


Regardless of other possible contributors to ice shelf instability not considered here (e.g., basal warming), föhn-induced surface melt and associated melt lakes were a likely trigger that pushed the LAIS past a structural tipping point. The estimated surface melt lake depth caused by the 9-day föhn melt event surpassed the critical melt lake depth of stability identified by model studies of the LBIS collapse and satellite-derived lake depths before the collapse of the LBIS (Banwell et al., 2013). The LAIS was likely the same thickness (200m) or thinner at the time of collapse so the estimate of critical surface lake depth for the LBIS that is applied to the LAIS may reflect an upper limit of melt lake depth of stability for the LAIS. Melt lake depth is likely underestimated because our estimation only accounts for melt during the 9-day melt event. Melt before this time period already exceeded an average melt year by 23% (118 mm w.e.) so melt lakes probably already existed. The large melt volume in a relatively short amount of time spatially expanded and increased melt lake formation and depth, filled crevasses, increased water pressure on the crevasse tip and walls and triggered large-scale hydrofracture cascades that led to catastrophic disintegration of the LAIS (Scambos et al., 2000; Banwell et al., 2013). The same cannot be said about the LBIS. Föhn-driven melt alone cannot convincingly explain the LBIS collapse in 2002 because föhn melt was even stronger in at least two prior seasons, 1992-93 and 1994-95. It is more likely that a combination of changes to LBIS structure (flow speed, suture zones, thinning), ocean forcing (ocean warming, sea ice loss, and wave action), and atmospheric forcing (precipitation, temperature, fohn winds), pushed it across a natural threshold of environmental factors and ultimately led LBIS to collapse.

5 Conclusions

The converging lines of evidence in these results show, for the first time, that observed and inferred föhn-driven melt is present in sufficient amounts, and at the right locations and times, to explain the disintegration of Larsen A in 1995 but not Larsen B in 2002. The fact that the LAIS and LBIS collapsed catastrophically within weeks and not through long-term thinning and retreat like other ice shelves (Prince Gustav, Wordie, George VI) suggests sudden disintegration is anomalous and requires forcings to match vulnerabilities (Scambos et al., 2003). We conclude that föhn wind-induced surface melt was a trigger for the collapse of the LAIS but not the LBIS. The remaining AP ice shelves may be more stable, at least from melt-driven instability, than previously thought. We have come to these conclusions with the following forms of evidence:

- First, both the LAIS and LBIS are impacted by powerful melt-inducing föhn jets that affect a large spatial portion of each ice shelf that reach the ice shelf terminus. Surface melt and melt lakes near the ice shelf terminus can lead to calving front collapse and structural instability for the remaining portion of the ice shelves (Pollard et al., 2015; Depoorter et al., 2013). Extant ice shelves are either not directly affected by a föhn jet, or are too vast to have any significant effect near the terminus.

https://doi.org/10.5194/tc-2021-301
Preprint. Discussion started: 25 October 2021
© Author(s) 2021. CC BY 4.0 License.


- Second, strong föhn winds were present prior to and at the time of collapse for the LAIS. This series of 3 föhn events lasted nine days total and produced over 25% of the total annual melt for the 1994/95 melt season. The enhanced melt, filled new and existing melt ponds above the critical (1 meter) melt lake depth of stability which ultimately triggered large-scale hydrofracture cascades and the LAIS collapse. A föhn event was also present at the onset of the LBIS collapse, however, melt rates were nominal and likely did not produce a trigger effect.
- Third, in the absence of föhn wind and concurrent melt, the surface liquid budgets of collapsed and intact ice shelves are climatically similar, which points to föhn winds as a driver of increased surface melt and possibly rapid collapse. The additional melt on the LAIS and LBIS compared to intact ice shelves created impermeable ice layers that support melt lake production, particularly when annual surface melt exceeds annual precipitation.

We acknowledge the subjectivity of labeling any of the causal factors that led to the LAIS or LBIS ice shelf collapses as a trigger when many factors contributed to the collapses. Nevertheless, this research clarifies the roles of föhn-induced melt for collapsed and extant ice shelves. Future forensic analyses of these ice shelf collapse events using advanced firn density models coupled with ice-ocean-atmospheric coupled simulations may be useful to better understand the role of surface melt in ice shelf instability. Further, the AP föhn wind regime has remained stable over the past half-century(Laffin et al., 2021) which points to enhanced surface temperatures and increased liquid phase precipitation as more important contributors to the future surface liquid budget on remaining ice shelves and is an important area of future research (Bozkurt et al., 2020). This research highlights a new understanding behind surface melt mechanisms for ice shelf collapse and suggests that extant ice shelves in the region may remain stable so long as surface liquid water from melt and precipitation remains within historical bounds.

Author contributions. M.K.L and C.S.Z designed the study. M.V.W. and S.M. curated the model simulation output and surface observations. M.K.L performed statistical data analysis. M.K.L. wrote the article with valuable input from all authors.

Competing interests. The authors declare no conflict of interest.

Acknowledgments. MKL was supported by the National Science Foundation (NRT-1633631) and NASA AIST (80NSSC17K0540). CSZ gratefully acknowledges support from the DOE BER ESM and SciDAC programs (DE-SC0019278, LLNL-B639667, LANL-520117). JMVW acknowledges support by PROTECT and was partly funded by the NWO (Netherlands Organisation for Scientific Research) VENI grant VI.Veni.192.083. We thank the Institute for Marine

https://doi.org/10.5194/tc-2021-301
Preprint. Discussion started: 25 October 2021
© Author(s) 2021. CC BY 4.0 License.


and Atmospheric research Utrecht (IMAU) for providing RACMO2 output. RACMO2 model data are available by request at https://www.projects.science.uu.nl/iceclimate/models/antarctica.php, however, a subset (2001-2018) of the data are hosted online at https://zenodo.org/record/3677642#.X-pXAFNKjUI.

References

Adusumilli, S., Fricker, H. A., Siegfried, M. R., Padman, L., Paolo, F. S. and Ligtenberg, S. R. M.: Variable Basal Melt Rates of Antarctic Peninsula Ice Shelves, 1994–2016, Geophys. Res. Lett., 45(9), 4086–4095, doi:10.1002/2017GL076652, 2018.

Alley, K. E., Scambos, T. A., Miller, J. Z., Long, D. G. and MacFerrin, M.: Quantifying vulnerability of Antarctic ice shelves to hydrofracture using microwave scattering properties, Remote Sens. Environ., 210, 297–306, doi:10.1016/j.rse.2018.03.025, 2018.

Banwell, A. F., MacAyeal, D. R. and Sergienko, O. V.: Breakup of the Larsen B Ice Shelf triggered by chain reaction drainage of supraglacial lakes, Geophys. Res. Lett., 40(22), 5872–5876, doi:10.1002/2013GL057694, 2013.

Banwell, A. F., Willis, I. C., Macdonald, G. J., Goodsell, B. and MacAyeal, D. R.: Direct measurements of ice-shelf flexure caused by surface meltwater ponding and drainage, Nat. Commun., 10(1), doi:10.1038/s41467-019-08522-5, 2019.

Bell, R. E., Banwell, A. F., Trusel, L. D. and Kingslake, J.: Antarctic surface hydrology and impacts on ice-sheet mass balance, Nat. Clim. Chang., 8(12), 1044–1052, doi:10.1038/s41558-018-0326-3, 2018.

Borstad, C., Khazendar, A., Scheuchl, B., Morlighem, M., Larour, E. and Rignot, E.: A constitutive framework for predicting weakening and reduced buttressing of ice shelves based on observations of the progressive deterioration of the remnant Larsen B Ice Shelf, Geophys. Res. Lett., 43(5), 2027–2035, doi:10.1002/2015GL067365, 2016.

Bozkurt, D., Bromwich, D. H., Carrasco, J., Hines, K. M., Maureira, J. C. and Rondanelli, R.: Recent Near-surface Temperature Trends in the Antarctic Peninsula from Observed, Reanalysis and Regional Climate Model Data, Adv. Atmos. Sci., 37(5), 477–493, doi:10.1007/s00376-020-9183-x, 2020.

Bozkurt, D., Bromwich, D. H., Carrasco, J. and Rondanelli, R.: Temperature and precipitation projections for the Antarctic Peninsula over the next two decades: contrasting global and regional climate model simulations, Clim. Dyn., doi:10.1007/s00382-021-05667-2, 2021.

Braun, M. and Humbert, A.: Recent retreat of wilkins ice shelf reveals new insights in ice shelf breakup mechanisms, IEEE Geosci. Remote Sens. Lett., 6(2), 263–267, doi:10.1109/LGRS.2008.2011925, 2009.

Depoorter, M. A., Bamber, J. L., Griggs, J. A., Lenaerts, J. T. M., Ligtenberg, S. R. M., Van Den Broeke, M. R. and Moholdt, G.: Calving fluxes and basal melt rates of Antarctic ice shelves, Nature, 502(7469), 89–92, doi:10.1038/nature12567, 2013.

Elvidge, A. D., Kuipers Munneke, P., King, J. C., Renfrew, I. A. and Gilbert, E.: Atmospheric Drivers of Melt on Larsen C

https://doi.org/10.5194/tc-2021-301
Preprint. Discussion started: 25 October 2021
© Author(s) 2021. CC BY 4.0 License.


Ice Shelf: Surface Energy Budget Regimes and the Impact of Foehn, J. Geophys. Res. Atmos., 125(17), doi:10.1029/2020JD032463, 2020.

Elvidge, A. D., Renfrew, I. A., King, J. C., Orr, A., Lachlan-Cope, T. A., Weeks, M. and Gray, S. L.: Foehn jets over the Larsen C Ice Shelf, Antarctica, Q. J. R. Meteorol. Soc., 141(688), 698–713, doi:10.1002/qj.2382, 2015.

Glasser, N. F. and Scambos, T. A.: A structural glaciological analysis of the 2002 Larsen B ice-shelf collapse, J. Glaciol., 54(184), 3–16, doi:10.3189/002214308784409017, 2008.

Glasser, N. F., Kulessa, B., Luckman, A., Jansen, D., King, E. C., Sammonds, P. R., Scambos, T. A. and Jezek, K. C.: Surface structure and stability of the Larsen C ice shelf, Antarctic Peninsula., 2009.

Gudmundsson, G. H.: Ice-shelf buttressing and the stability of marine ice sheets, Cryosphere, 7(2), 647–655, doi:10.5194/tc-7-647-2013, 2013.

Kuipers Munneke, P., Van Den Broeke, M. R., King, J. C., Gray, T. and Reijmer, C. H.: Near-surface climate and surface energy budget of Larsen C ice shelf, Antarctic Peninsula, Cryosphere, 6(2), 353–363, doi:10.5194/tc-6-353-2012, 2012.

Laffin, M. K., Zender, C. S., Singh, S., Van Wessem, J. M., Smeets, C. J. P. P. and Reijmer, C. H.: Climatology and Evolution of the Antarctic Peninsula Föhn Wind-Induced Melt Regime From 1979–2018, J. Geophys. Res. Atmos., 126(4), doi:10.1029/2020JD033682, 2021.

Leeson, A. A., Van Wessem, J. M., Ligtenberg, S. R. M., Shepherd, A., Van Den Broeke, M. R., Killick, R., Skvarca, P., Marinsek, S. and Colwell, S.: Regional climate of the Larsen B embayment 1980-2014, J. Glaciol., 63(240), 683–690, doi:10.1017/jog.2017.39, 2017.

Mahaffy, P. R., Webster, C. R., Atreya, S. K., Franz, H., Wong, M., Conrad, P. G., Harpold, D., Jones, J. J., Leshin, L. A., Manning, H., Owen, T., Pepin, R. O., Squyres, S. and Trainer, M.: Abundance and isotopic composition of gases in the martian atmosphere from the Curiosity rover, Science (80)., 341(6143), 263–266, doi:10.1126/science.1237966, 2013.

Massom, R. A., Scambos, T. A., Bennetts, L. G., Reid, P., Squire, V. A. and Stammerjohn, S. E.: Antarctic ice shelf disintegration triggered by sea ice loss and ocean swell, Nature, 558(7710), 383–389, doi:10.1038/s41586-018-0212-1, 2018.

Mattia Poinelli, I., Schodlok, M. and Larour, E.: Modeling of Ocean Dynamics in Ice-Shelf Rifts, ESSOAr, doi:10.1002/essoar.10506246.2, 2021.

McGrath, D., Steffen, K., Holland, P. R., Scambos, T., Rajaram, H., Abdalati, W. and Rignot, E.: The structure and effect of suture zones in the Larsen C Ice Shelf, Antarctica, J. Geophys. Res. Earth Surf., 119(3), 588–602, doi:10.1002/2013JF002935, 2014.

Mulvaney, R., Abram, N. J., Hindmarsh, R. C. A., Arrowsmith, C., Fleet, L., Triest, J., Sime, L. C., Alemany, O. and Foord, S.: Recent Antarctic Peninsula warming relative to Holocene climate and ice-shelf history, Nature, 489(7414), 141–144, doi:10.1038/nature11391, 2012.

https://doi.org/10.5194/tc-2021-301
Preprint. Discussion started: 25 October 2021
© Author(s) 2021. CC BY 4.0 License.


Polashenski, C., Golden, K. M., Perovich, D. K., Skyllingstad, E., Arnsten, A., Stwertka, C. and Wright, N.: Percolation blockage: A process that enables melt pond formation on first year Arctic sea ice, J. Geophys. Res. Ocean., 122(1), 413–440, doi:10.1002/2016JC011994, 2017.

Pollard, D., DeConto, R. M. and Alley, R. B.: Potential Antarctic Ice Sheet retreat driven by hydrofracturing and ice cliff failure, Earth Planet. Sci. Lett., 412, 112–121, doi:10.1016/j.epsl.2014.12.035, 2015.

Pritchard, H. D., Ligtenberg, S. R. M., Fricker, H. A., Vaughan, D. G., Van Den Broeke, M. R. and Padman, L.: Antarctic ice-sheet loss driven by basal melting of ice shelves, Nature, 484(7395), 502–505, doi:10.1038/nature10968, 2012.

Qiao, G., Li, Y., Guo, S. and Ye, W.: Evolving instability of the scar inlet ice shelf based on sequential landsat images spanning 2005-2018, Remote Sens., 12(1), doi:10.3390/RS12010036, 2020.

Rignot, E., Casassa, G., Gogineni, P., Krabill, W., Rivera, A. and Thomas, R.: Accelerated ice discharge from the Antarctic Peninsula following the collapse of Larsen B ice shelf, Geophys. Res. Lett., 31(18), doi:10.1029/2004GL020697, 2004.

Robel, A. A. and Banwell, A. F.: A Speed Limit on Ice Shelf Collapse Through Hydrofracture, Geophys. Res. Lett., 46(21), 12092–12100, doi:10.1029/2019GL084397, 2019.

Rott, H., Rack, W., Nagler, T. and Skvarca, P.: Climatically induced retreat and collapse of norther Larsen Ice Shelf, Antarctic Peninsula, Ann. Glaciol., 27, 86–92, doi:10.3189/s0260305500017262, 1998.

Sandhäger, H., Rack, W. and Jansen, D.: Model investigations of Larsen B Ice Shelf dynamics prior to the breakup. [online] Available from: http://www.uib.no/People/ngfls/frisp/Rep16/sandhageretal.pdf, 2005.

Scambos, T. A., Hulbe, C., Fahnestock, M. and Bohlander, J.: The link between climate warming and break-up of ice shelves in the Antarctic Peninsula, J. Glaciol., 46(154), 516–530, doi:10.3189/172756500781833043, 2000.

Scambos, T., Hulbe, C. and Fahnestock, M.: Climate-Induced Ice Shelf Disintegration in the Antarctic Peninsula, pp. 79–92., 2013.

Schodlok, M. P., Menemenlis, D. and Rignot, E. J.: Ice shelf basal melt rates around Antarctica from simulations and observations, J. Geophys. Res. Ocean., 121(2), 1085–1109, doi:10.1002/2015JC011117, 2016.

Trusel, L. D., Frey, K. E., Das, S. B., Karnauskas, K. B., Kuipers Munneke, P., Van Meijgaard, E. and Van Den Broeke, M. R.: Divergent trajectories of Antarctic surface melt under two twenty-first-century climate scenarios, Nat. Geosci., 8(12), 927–932, doi:10.1038/ngeo2563, 2015.

Trusel, L. D., Frey, K. E., Das, S. B., Munneke, P. K. and Van Den Broeke, M. R.: Satellite-based estimates of Antarctic surface meltwater fluxes, Geophys. Res. Lett., 40(23), 6148–6153, doi:10.1002/2013GL058138, 2013.

Van den Broeke, M.: Strong surface melting preceded collapse of Antarctic Peninsula ice shelf, Geophys. Res. Lett., 32(12), 1–4, doi:10.1029/2005GL023247, 2005.

Vaughan, D. G., Marshall, G. J., Connolley, W. M., Parkinson, C., Mulvaney, R., Hodgson, D. A., King, J. C., Pudsey, C. J. and Turner, J.: Recent rapid regional climate warming on the Antarctic Peninsula, Clim. Change, 60(3), 243–274,

https://doi.org/10.5194/tc-2021-301
Preprint. Discussion started: 25 October 2021
© Author(s) 2021. CC BY 4.0 License.


doi:10.1023/A:1026021217991, 2003.